Civil Engineering and Architecture 13(6): 4099-4111, 2025 http://www.hrpub.org
DOI: 10.13189/cea.2025.130601

Analytical and Finite Element Characterisation of a Randomly Reinforced Recyclable Composite for Reinforcing Aged Concrete Slabs

Sofiene Helaili[1,2,*], Yosra Zaouali[3], Moez Chafra[4,5]

[1]Tunisia Polytechnic School, Carthage University, LASMAP (LR03ES06), Rue El-Khawarizmi, BP 743, 2078, La Marsa, Tunisia
[2]ISTEUB, Carthage University, 2 Rue de l'Artisanat Charguia 2, 2035, Tunis, Tunisia
[3]IMECA-SARL R&D, Tunis, Tunisia
[4]Tunis EL Manar University, Campus Universitaire, B. P 244, Tunis 2092, Tunisia
[5]Matériaux, Optimisation et Energie pour la Durabilité (LR-MOED-ENIT),
Tunis EL Manar University, Campus Universitaire, BP 244, Tunis 2092, Tunisia

Received December 27, 2024; Revised July 7, 2025; Accepted October 14, 2025

Cite This Paper in the Following Citation Styles

(a): *[1] Sofiene Helaili, Yosra Zaouali, Moez Chafra , "Analytical and Finite Element Characterisation of a Randomly Reinforced Recyclable Composite for Reinforcing Aged Concrete Slabs," Civil Engineering and Architecture, Vol. 13, No. 6, pp. 4099 - 4111, 2025. DOI: 10.13189/cea.2025.130601.*

(b): *Sofiene Helaili, Yosra Zaouali, Moez Chafra (2025). Analytical and Finite Element Characterisation of a Randomly Reinforced Recyclable Composite for Reinforcing Aged Concrete Slabs. Civil Engineering and Architecture, 13(6), 4099 - 4111. DOI: 10.13189/cea.2025.130601.*

Abstract Using fibers generally necessitates sorting and, in some cases, chemical treatments, which raises manufacturing costs and has a negative impact on the environment. This problem is solved by using a random distribution of short, disorganized fibers. To use randomly dispersed short natural fibers, the mechanical properties of the randomly reinforced composite must be estimated. Two analytical models and one finite element model were used to analyze composites reinforced with short fibers. Calcium Carbonate Precipitate ($CaCO_3$) and PolyVinyl Chloride (C_2H_4Cl)n composites are being investigated as potential applications in the building industry reinforcement. The CCP improves recyclability while lowering petrochemical and energy consumption during production, thereby lowering the carbon footprint. The Mori-Tanaka model, the Halpin-Tsai model, and a finite element technique model were used to investigate the effects of distribution on the mechanical properties of the composite. The first is the effect of fiber volume fraction on the elastic mechanical properties of the composite. Elastic moduli increased by 97 percent for the Mori-Tanaka model, 101 percent for the Halpin-Tsai model, and 74 percent for the finite element technique model, as fiber content increased from 9 to 45 percent. The second factor is the impact of fiber orientation on a specific volume fraction. In comparison to a composite with uniform fiber concentration across all orientations, the elastic characteristics vary by 15.56 percent when the fiber concentration in each orientation is changed. This finding implies that the random distribution of fibers has no discernible effect on mechanical properties. The length of the fiber changes the stiffness by approximately 6.64 percent, depending on the concentration. This stiffness fluctuation is observed until the fiber's aspect ratio reaches 100; the rise becomes negligible after that. The fund mechanical properties were injected into a slab flexion finite element model to simulate the deformation of the un-reinforced and reinforced concrete slab with recyclable composites. The deflexion of the slab is reduced, and concrete slabs can be reinforced with sur composites.

Keywords Halpin-Tsai, Mechanical Properties, Mori-Tanaka, Recyclability, Slab Aging Reinforcement

1. Introduction

Recent research has shown that the carbon footprint of building materials is a major concern. To address this, natural and recyclable materials [1] are increasingly used to create composites that are friendly to the environment. The lifecycle of buildings [2] is studied to assess the potential for recycling primary building materials. Similarly, the lifecycle of infrastructure equipment, particularly the recycling potential of certain materials, has also been examined [3]. Short-fiber composites can be rapidly produced and exhibit excellent mechanical properties [4], [5]. Since the mixture of short fibers and plastic matrix can be processed via injection, extrusion, or compression molding, it is possible to produce complex-shaped components. Moreover, organizing short fibers as reinforcements in an organized manner can provide more suitable properties, thereby enhancing stiffness/strength throughout the thickness. Determining the composite material's mechanical properties, composed of a statistically isotropic random distribution of isotropic and elastic short cylindrical fibers embedded in a continuous and isotropic matrix, is a classic problem in solid mechanics, commonly addressed through homogenization [6]. This process is performed on the components' mechanical properties and geometric shapes. In unidirectional composites, the modulus in the fiber axis direction is greater than the modulus in the transverse direction.

Consequently, these materials are used in applications [7], [8], [9], [10], [11] where the stress distribution can be precisely determined. However, in applications where the state of stress cannot be predicted or is not approximately equal in all directions, unidirectional laminates may not be the best option; therefore, a short-fiber composite provides a suitable alternative. Several studies [12], [13], [14], [15], [16], [17] have examined the reinforcement of PolyVinyl Chloride (PVC) with various fillers. According to reference [18], renewable resource materials are gaining importance in a world where the price of crude oil and carbon dioxide (CO_2) emissions are rising; conventional plastics have reached a price point and a questionable reputation that encourages the search for alternatives. Natural fibers are renewable natural resources, biodegradable and recyclable at the end of their useful life. Good candidates include composites typically filled or reinforced with plant fibers and plastics such as PolyVinyl Chloride. Mechanical properties of various wood fiber arrangements [19], processing technique and fiber orientation angle of wood fibers [20], properties of extruded rigid PVC/wood-flour composites [21], and morphological properties of sandwich composites of wood/PVC and glass fiber/PVC layers [22] were investigated. This study expands the understanding of PVC composites. The primary goal is to predict the effect of fiber volume fraction, fiber orientation distribution, and fiber length distribution on the homogenized elastic moduli of Calcium Carbonate Precipitate CCP/PVC PolyVinyl Chloride composites. CCP/PVC can serve as a matrix for other composites; consequently, its mechanical properties must be determined. Short-fiber composites are composites that contain short fibers for reinforcement. These composites are also known as discontinuous fiber-reinforced composites [23]. The composite behavior of a short fiber composite with randomly oriented fibers in a polymer matrix is isotropic [24].

Additionally, various studies have explored the effects of different fibers and fillers, such as recycled fibers [25], banana, palm leaf sheath fibers [26], nano-silica, micro-steel fibers, silica fume [27], metal oxide [28], keratin[29], and aggregates such as granite [30], [31] on ultra-high-performance concrete. Compressive strength of 180.6 MPa was achieved using Ilmenite aggregate and steel fiber, and the best radiation protection properties were achieved using lead fiber and magnetite aggregates. According to Ghanim et al. [32], adding 0.4% glass fiber to lightweight concrete maintained a good compressive strength.

This paper can contribute to a greater comprehension of the mechanical properties of randomly reinforced composites and aid in developing construction materials with enhanced properties and recyclability. This study focuses specifically on the effects of fiber volume fraction, fiber orientation, and fiber length on the mechanical properties of the composite, which can contribute to evaluating the recycling potential of the primary building materials, a current concern in the construction materials field. Reusing and recycling construction materials reduces environmental impact.

This study introduces a novel approach to predicting the homogeneous elastic moduli of Calcium Carbonate Precipitate CCP/PVC PolyVinyl Chloride composites by analyzing the effects of fiber volume fraction, fiber orientation distribution, and fiber length distribution. While previous research has explored fiber reinforced PVC composites, the specific influence of these parameters on the mechanical properties of CCP/PVC remains insufficiently studied. By integrating homogenization techniques, this work provides new insights into the mechanical properties identification of CCP/PVC composite, which can serve as a basis for optimal use in sustainable construction materials.

2. Materials and Methods

2.1. Matrix and Fibers Materials

The investigated material belongs to the random composite with short fibers family. The matrix is rigid and composed of PolyVinyl Chloride (PVC) with the formula $(C_2H_2Cl)n$, where n is the degree of polymerization (See Figure 1). The fibers consist of Calcium Carbonate Precipitate (CCP) with the formula $CaCO_3$.

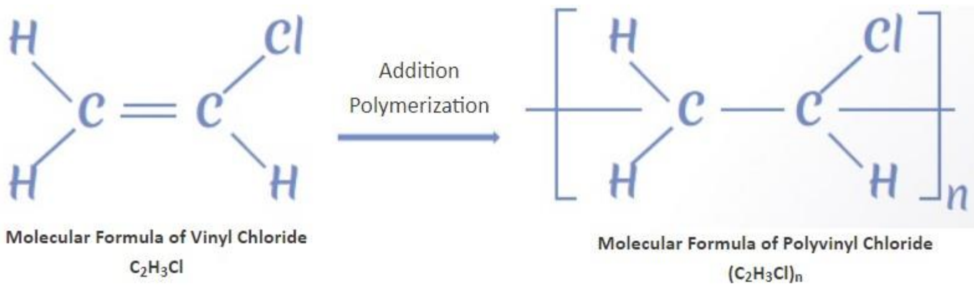

Figure 1. Structural formula of PolyVinyl Chloride (PVC) (C_2H_2Cl)n

PVC is the third-most-produced thermoplastic polymer after polyethylene and polypropylene. PVC is durable, cheap, and easy to assemble, so over half of it is used in construction. Phthalates are the most common plasticizers for PVC. This material is used to manufacture flexible hoses, tubing, flooring, roofing membranes, and cable insulation. In addition to figurines and inflatable products such as waterbeds, pool toys, and inflatable structures, PVC is also commonly used in figurines.

Calcium Carbonate Precipitate (CCP), composition indicated on Figure 2, is a manufactured substance derived from the decomposition and resynthesis of pure limestone. Depending on the application, they can enhance properties like strength, impact resistance, and abrasion resistance. CCP is one of the most popular fillers in the plastics industry, and its use reduces the environmental impact of the plastics industry. Adding calcium carbonate to plastic matrices has resulted in increased performance [33], enhanced processing, and enhanced sustainability of the final product while reducing greenhouse gas emissions, petrochemical consumption, and energy consumption.

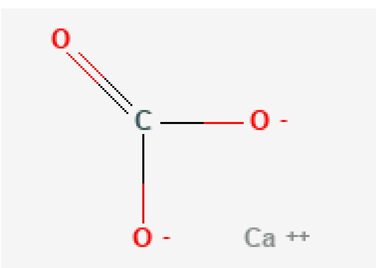

Figure 2. Structural formula of Calcium Carbonate Precipitate (CCP)

The elastic mechanical properties are listed in Table 1.

Table 1. PVC and CCP mechanical properties

Material	**PVC Matrix [34]**	**CCP Fibers [35]**
Young's modulus (GPa)	2.631	20.000
Poisson's ratio	0,35	0,36

2.2. Halpin-Tsai Model

The Halpin–Tsai model [36] established a simple and generalized semi-empirical equation for approximating fiber-reinforced composites' longitudinal and transverse moduli. The Halpin-Tsai equations can be written as follows:

$$E_L = E_m\left(\frac{1+(2l/d)\eta_L V_f}{1-\eta_L V_f}\right) \tag{1}$$

And

$$E_T = E_m\left(\frac{1+2\eta_T V_f}{1-\eta_T V_f}\right) \tag{2}$$

η_L *and* η_T are given in equation (3) and equation (4) :

$$\eta_L = \frac{\frac{E_f}{E_m}-1}{\frac{E_f}{E_m}+2\frac{l}{d}} \tag{3}$$

$$\eta_T = \frac{\frac{E_f}{E_m}-1}{\frac{E_f}{E_m}+2} \tag{4}$$

Where:

- η_L: is the longitudinal ratio
- η_T: is the transversal ratio
- V_f: is the fiber volume fraction
- l: fiber length
- d: fiber diameter
- E_m: matrix elastic modulus
- E_f: fiber elastic modulus

Randomly oriented short-fiber composites are produced to obtain composites with essentially isotropic properties in a plane [37]. The elastic modulus E_{comp} (refer to equation (5)) and shear modulus G_{comp} (refer to equation (6)) can be calculated as follows:

$$E_{comp} = \frac{3}{8}E_L + \frac{5}{8}E_T \tag{5}$$

$$G_{comp} = \frac{1}{8}E_L + \frac{2}{8}E_T \tag{6}$$

2.3. Mori-Tanaka Model

Micro-mechanical models connect two scales of material description: a microscopic scale associated with material heterogeneities and a macroscopic scale corresponding to the structure's scale. Heterogeneities influence the material's macroscopic behavior. To predict the mechanical composite properties, the micro-macro transition principle defines a fictitious homogeneous material equivalent to an actual heterogeneous material. For two phases of the unidirectional composite, the following hypotheses are applied:

- the fiber and the matrix are linear, elastic, and isotropic,
- fibers are axisymmetric, identical in size and shape, and characterized by a ratio of form equal to l/d,
- fiber and matrix are interfaces that are tied.

The tensor of strain localization A^{MT} (see Eq. (7) and Eq. (8)) for the Mori-Tanaka model is expressed as follows:

$$A^{MT} = A^{E}\left[\left(1 - v_f\right)I + v_f A^{E}\right]^{-1} \tag{7}$$

$$A^{E} = [(I + E^{\mathrm{E}}{:}\, S^{m}(C^{f} - C^{m})]^{-1} \tag{8}$$

Where,

- A^E is the Eshelby tensor of strain localization,
- I is the identity matrix,
- E^E is the Eshelby tensor,
- S^m is the flexibility matrix of the composite matrix,
- C^m is the stiffness matrix of the composite matrix,
- C^f is the stiffness matrix of the fibers.

2.4. Numerical Homogenization Approach

ANSYS Multiphysics commercial finite element code is used for the finite element model. Periodicity can be observed when observing the structure of random composite with short fibers (see Figure 3, [38]). A periodic structure can be represented by one element named Representative Elementary Volume (REV). Thus, studying the REV can give the homogenized coefficients of a composite.

For an orthotropic material, the stiffness matrix has the following form:

$$[C] = \begin{pmatrix} C_{11} & C_{12} & C_{13} & 0 & 0 & 0 \\ C_{12} & C_{22} & C_{23} & 0 & 0 & 0 \\ C_{13} & C_{23} & C_{33} & 0 & 0 & 0 \\ 0 & 0 & 0 & C_{44} & 0 & 0 \\ 0 & 0 & 0 & 0 & C_{55} & 0 \\ 0 & 0 & 0 & 0 & 0 & C_{66} \end{pmatrix} \tag{9}$$

To determine the homogenized stiffness matrix C (see Eq. (9)), three tensile tests in each direction and three shear tests in each direction [39] are applied. After applying these six tests, we can compute all components of the stiffness matrix S (see Eq. (10)) and then determine the elastic moduli of the material given by the following matrix form:

$$[S] = [C^{-1}] = \begin{pmatrix} \frac{1}{E_x} & \frac{-\upsilon_{yx}}{E_y} & \frac{-\upsilon_{zx}}{E_z} & 0 & 0 & 0 \\ \frac{-\upsilon_{xy}}{E_x} & \frac{1}{E_y} & \frac{-\upsilon_{zy}}{E_z} & 0 & 0 & 0 \\ \frac{-\upsilon_{xz}}{E_x} & \frac{-\upsilon_{yz}}{E_y} & \frac{1}{E_z} & 0 & 0 & 0 \\ 0 & 0 & 0 & \frac{1}{2G_{yz}} & 0 & 0 \\ 0 & 0 & 0 & 0 & \frac{1}{2G_{zx}} & 0 \\ 0 & 0 & 0 & 0 & 0 & \frac{1}{2G_{xy}} \end{pmatrix} \tag{10}$$

For example, to determine C_{11} and then E_x , a deformation ϵ_x equal to 1 is applied in the x-direction. The resulting numerical stress σ_x is equal to C_{11}. Then, E_x can be determined.

2.5. Simulation Data

Figure 4 depicts a CCP/PVC composite plate with random reinforcing. The fibers have a cylindrical shape. In the matrix, the fibers are distributed in nine directions (= -90, -60, -45, -30, 0, 30, 45, 60, and 90). Variations are made to the fiber concentration per orientation and total fiber volume fraction Vf. The effect of variation on composite elastic moduli is studied.

There are nine cases generated. Table 2 lists case numbers 1 through 6 and the numbers 4.2, 4.3, and 4.4. From case, N°1 to case N°6, the total fiber volume fraction Vf rises from 9% to 45%. The Vf is distributed equally in all nine directions. For cases 4, 4.2, 4.3, and 4.4, the total volume fraction of fibers Vf equals 28 percent, but the concentration of fibers is not uniformly distributed in the nine directions.

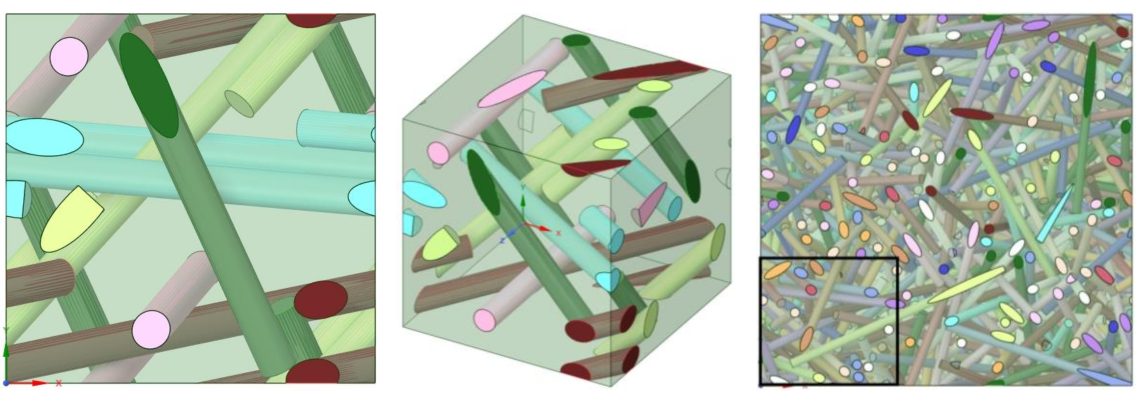

(a) (b) (c)

Figure 3. Generation of randomly distributed short fibers: (a) plane view of fibers in the matrix, (b) isometric 3D view of the RVE, (c) RVE in the composite

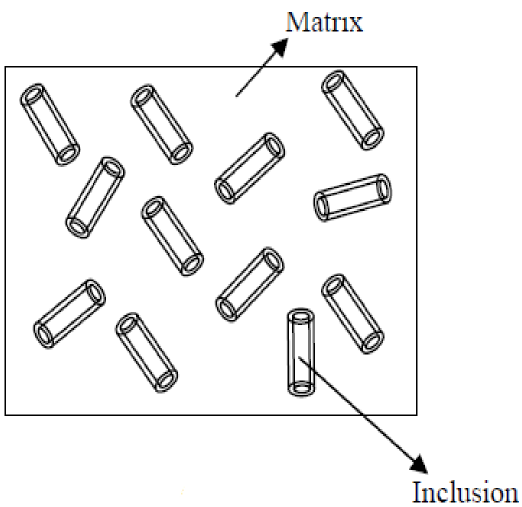

Figure 4. Model of randomly reinforced composite with short cylindrical fibers

Table 2. Simulation cases: volume fibers repartition function of orientation and total fibers volume fraction Vf

Vf at θ / Case N °	**1**	**2**	**3**	**4**	**5**	**6**	**4.2**	**4.3**	**4.4**
-90 °	1%	1,5%	2,5%	3,11%	4%	5%	4,67%	0%	28%
-60 °	1%	1,5%	2,5%	3,11%	4%	5%	4,67%	0%	0%
-45 °	1%	1,5%	2,5%	3,11%	4%	5%	0%	7%	0%
-30 °	1%	1,5%	2,5%	3,11%	4%	5%	0%	0%	0%
0 °	1%	1,5%	2,5%	3,11%	4%	5%	0%	7%	0%
30 °	1%	1,5%	2,5%	3,11%	4%	5%	9,33%	0%	0%
45 °	1%	1,5%	2,5%	3,11%	4%	5%	4,67%	7%	0%
60 °	1%	1,5%	2,5%	3,11%	4%	5%	4,67%	0%	0%
90 °	1%	1,5%	2,5%	3,11%	4%	5%	0%	7%	0%
Total Vf	9%	14%	23%	28%	36%	45%	28%	28%	28%

The nine fiber orientations listed in Table 2 (-90 °, -60 °, -45 °, -30 °, 0 °, 30 °, 45 °, 60 ° and 90 °) are all measured in the same 2D plane, representing the in-plane angular directions of the cylindrical fibers. This assumption reflects the planar isotropy typical of short-fiber reinforced composites and allows for a simplified yet representative model of fiber distribution in real-world manufacturing. Regarding the angle plane, since the study focuses on in-plane mechanical properties and aims to maintain a statistically isotropic distribution, all angles are considered within a single plane parallel to the composite plate.

A mesh convergence study was conducted to assure accurate homogenized properties without excessive computational cost. The mesh density was incrementally refined until changes in the calculated elastic moduli fell below 2%. The final mesh configuration provided a balance between precision and computational efficiency, and the selected mesh size and element type are now described in Section 2.4 of the revised manuscript.

2.6. Aged Concrete Slab Reinforcement

2.6.1. Geometry

The studied concrete slabs are 1x1 meter square dimensions (see Figure 5). The CCP/PVC layer is applied on the lower surface of the slab to reinforce the slab against the flexion. The slab thickness is 20 cm, and the thickness of the CCP/PVC layer is 3 cm.

2.6.2. Material Properties

Two materials are used in this study: concrete and CCP/PVC. The elasticity moduli and the traction and compression strengths are indicated in Table 3. The Young modulus of the concrete varies from 40 GPa to 28 GPa to simulate the aging of the slab. The Young modulus of the CCP/PVC composite varies from 3.5 GPa to 6.431 GPa and Poisson’s ratio from 0.45 to 0.6. The values of CCP/PVC properties are those of the Finite Element Method and are detailed for each case in Table 4.

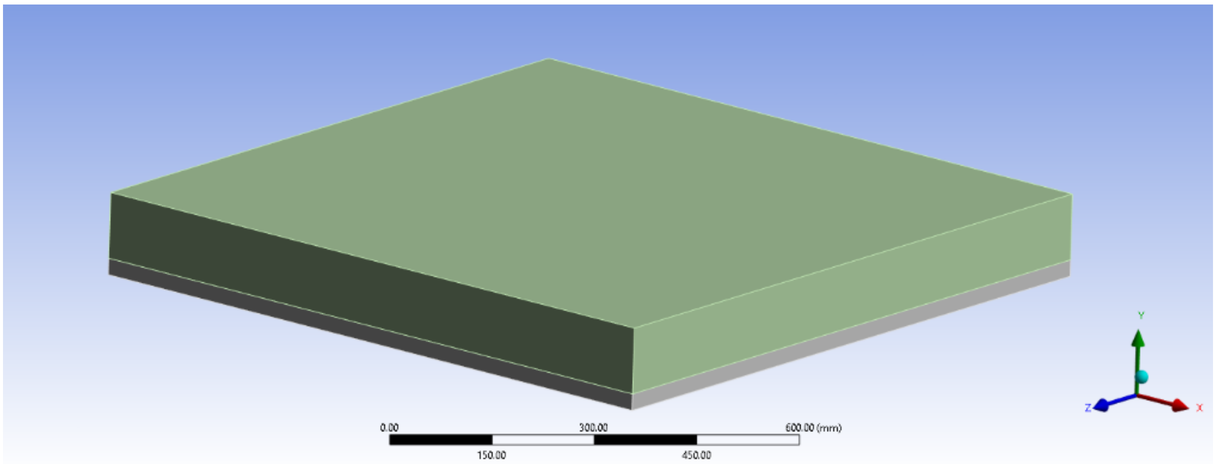

Figure 5. Concrete slab reinforced with CCP/PVC layer

Table 3. Mechanical properties

Parameters	Concrete	CCP/PVC
Young Modulus E (GPa)	[40-20]	[3.500-6.341]
Poisson's ratio	0.20	[0.45-0.60]

Table 4. Simulation results for Mori-Tanaka, Halpin-Tsai, and FEM models

Case	**Mori-Tanaka**				**Halpin-Tsai**				**Finite Element Method**			
N °	**E_L (GPa)**	**E_T (GPa)**	**G_{LT} (GPa)**	**v_{LT}**	**E_L (GPa)**	**E_T (GPa)**	**G_{LT} (GPa)**	**v_{LT}**	**E_L (GPa)**	**E_T (GPa)**	**G_{LT} (GPa)**	**v_{LT}**
1	3,562	3,634	1,252	0,48	3,252	3,293	1,243		3,624	3,610	1,165	0,48
2	3,903	3,902	1,365	0,49	3,593	3,659	1,357		3,500	3,512	1,365	0,49
3	4,559	4,559	1,640	0,49	4,489	4,489	1,628		4,497	4,497	1,616	0,49
4	5,085	5,085	1,797	0,46					5,100	5,096	1,779	0,45
4.2	5,176	5,176	1,897	0,49					5,185	5,196	1,836	0,49
4.3	5,239	5,007	1,754	0,49					5,266	5,000	1,743	0,49
4.4	4,578	5,900	1,716	0,45					4,442	5,889	1,723	0,44
5	5,978	6,000	2,148	0,49	5,513	5,585	2,096		4,584	5,023	2,261	0,49
6	7,000	7,024	2,539	0,49	6,535	6,537	2,461		6,288	6,341	2,670	0,49

2.6.3. Finite Element Model

The finite element model is developed by Ansys. The Design Points technique is used to vary the material properties and extract results from a parametric finite element model. The nine cases material properties are used with a varying Young's modulus of the concrete. The slab is subject to 1 ton. The equivalent surface load is 1 ton per square meter. The concrete slab is modeled as simply supported on all four edges, simulating realistic support conditions for structural applications. This boundary setup allows vertical displacement while preventing in-plane translations, ensuring accurate representation of slab deformation under loading. A uniformly distributed load equivalent to 1 ton/m^2 is applied on the top surface of the slab to simulate service-level structural loading conditions. A mesh convergence analysis was conducted by refining the element size incrementally. The final mesh was selected when further refinement resulted in less than 2% variation in key results such as maximum deflection and stress values. This ensures that numerical results are reliable without introducing unnecessary computational overhead.

3. Results and Discussion

Using the Mori-Tanaka, Halpin-Tsai, and finite element method models, the longitudinal, transversal, and shear moduli are calculated for all cases. Results are detailed in Table 4.

3.1. Effect of Volume Fraction of Orientation

Fiber orientation is fixed to determine how the orientation volume fraction affects the homogenized elastic moduli. Fibers are evenly distributed in these orientations: 0, 30, 45, 60, and 90. (see Table 2). Cases 1–6. All orientations increase volume fraction from 0.09 to 0.45 equally. Table 3 shows that an isotropic composite has the same volume fraction of fibers in all orientations. Randomly reinforced plastic composites [40]and heterogeneous composite soils [41] show that longitudinal EL and transverse ET moduli are equal.

The composite's elastic modulus and shear modulus increase if the CCP fiber volume fraction is increased while maintaining orientations. Case 1 has 3,634 MPa elastic moduli and 9% fiber volume fraction. Six has a volume fraction of 45% and an elastic modulus of 7 MPa. The moduli do not increase linearly with fiber volume fraction: a fivefold increase in CCP concentration from 9 percent to 45 percent doubles stiffness (See Table 4).

3.2. Effect of Fiber Orientation Distribution

For cases N°4–Cas N°4.4, the fiber volume fraction is kept at 28% to observe the effect of fiber orientation distribution on homogenized elastic moduli. Each orientation has variable volume fractions. Short fiber composites' mechanical properties depend heavily on fiber orientation. Table 3 shows that fiber orientation determines composite mechanical properties. CCP fiber reinforcement increases elastic moduli in one direction more than the other as fiber volume fraction increases. Thus, random composites with controllable mechanical properties have applications.

3.3. Effect of Fiber Length Distribution

To illustrate the effect of fiber length distribution on homogenized elastic moduli, the aspect ratio of fiber, and length over fiber diameter, varied between 25 and 400. Three fiber volume fractions are employed: 9%, 22.5 %, and 45%. (See Table 5).

Table 5. Effect of the aspect ratio of fiber on the longitudinal modulus E_L

l/d	E_L (GPa) Vf = 9%	E_L (GPa) Vf = 22,5%	E_L (GPa) Vf = 45%
25	4,02	6,19	9,93
50	4,11	6,37	10,18
75	4,16	6,46	10,27
100	4,20	6,51	10,32
200	4,25	6,55	10,41
300	4,25	6,58	10,43
400	4,25	6,60	10,46

The Young's modulus E_L increases with fiber length (see Figure 6) until l/d=100, at which point the modulus approaches an asymptotic value.

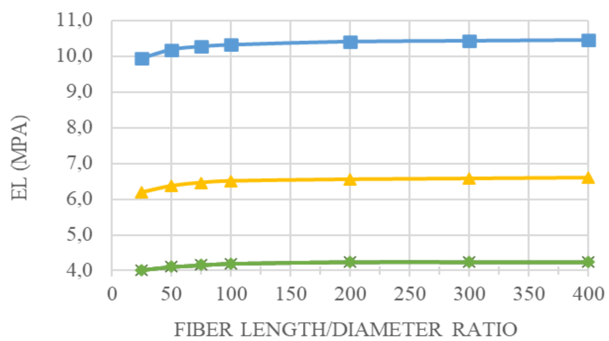

Figure 6. Effect of the aspect ratio of fiber on the longitudinal modulus E_L for different fiber concentrations

The analysis of the effect of the type of fiber length distribution on the mechanical properties reveals that the random distribution of fiber length in case N°4.1 results in greater Young's and shear moduli than the equally distributed configuration in case N4.

3.4. Effect of CCV/PVC Composite Plates on Aged Plate Reinforcement

The slab is simply supported and subject to deflexion. Figure 7 and Figure 8 present the total deformation and the maximal principal stresses. The deformation of the non-reinforced and the reinforced slab deformation are indicated in Figure 7(a) and Figure 7(b) respectively. Figure 8 (a), (b), (c) and (d) presents respectively the tension stress for non-reinforced slab, reinforced slab, the concrete part of the reinforced slab and the composite part of the reinforced slab.

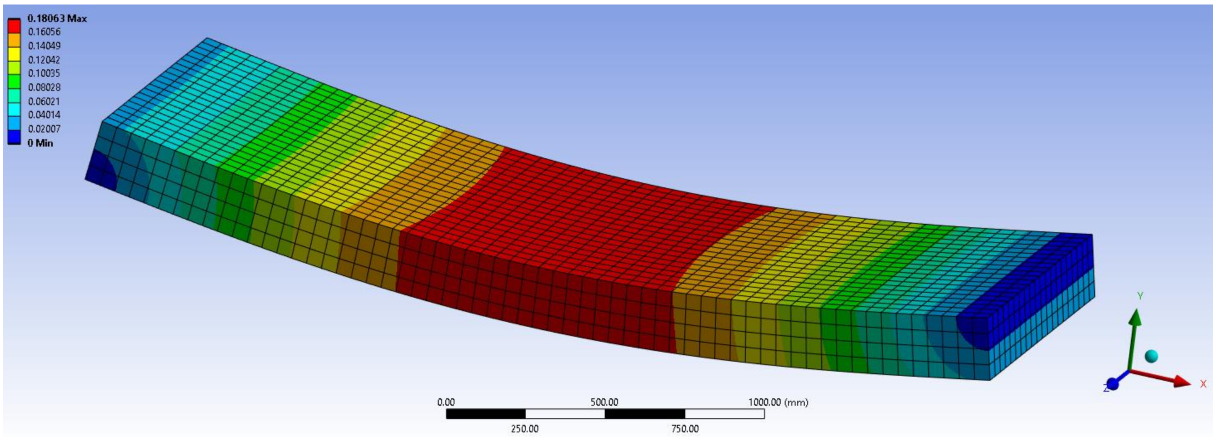

(a) Non-reinforced Slab Deflexion

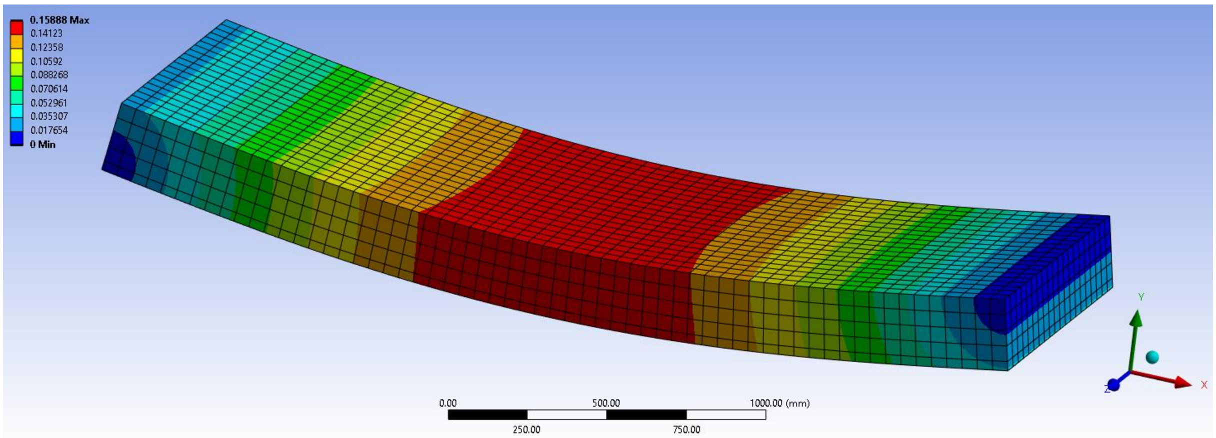

(b) Reinforced Slab Deflexion

Figure 7. Deformation

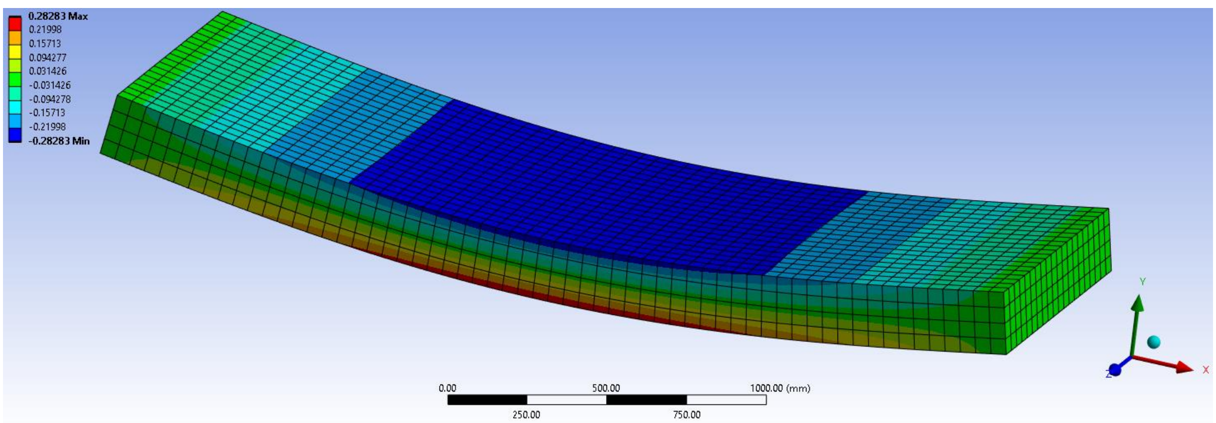

(a) Non-reinforced slab tension stress

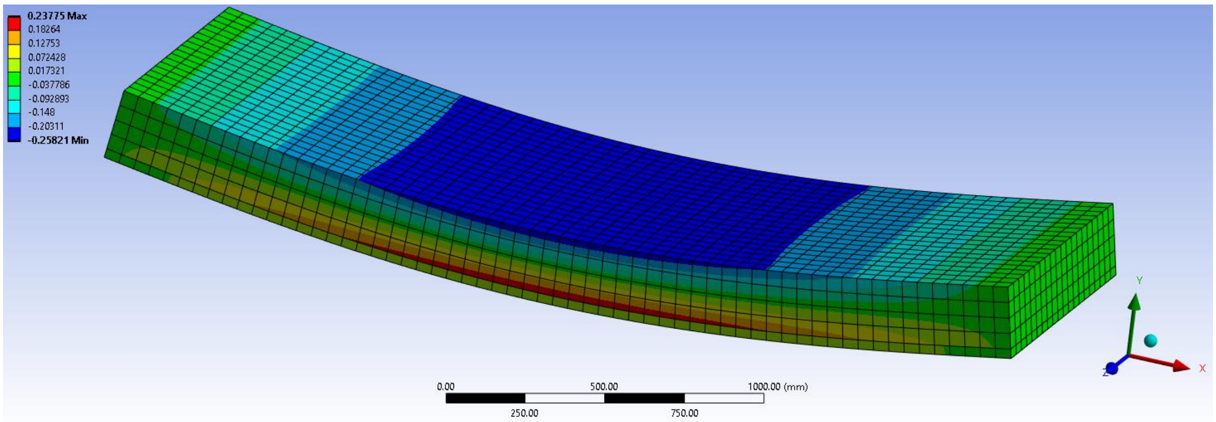

(b) Reinforced slab tension stress

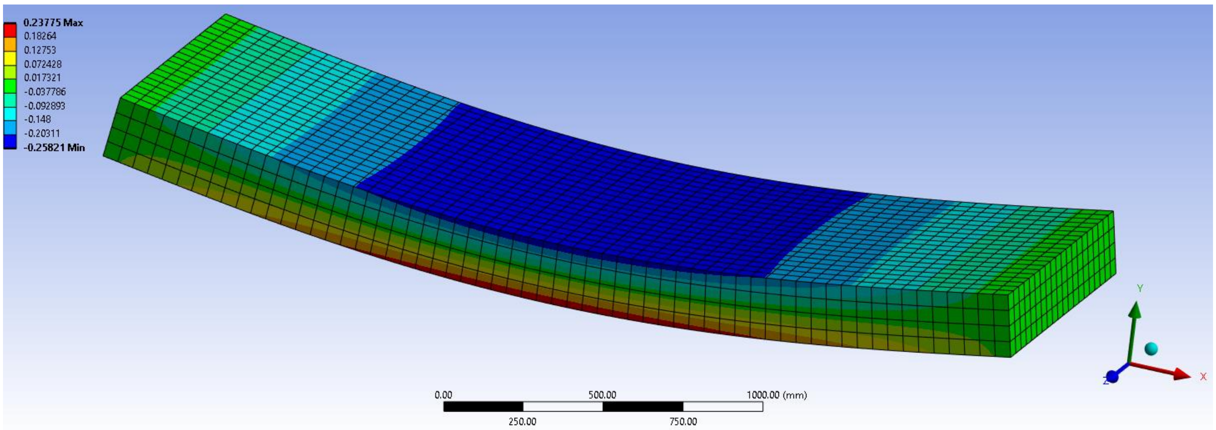

(c) Concrete part of Reinforced slab tension stress

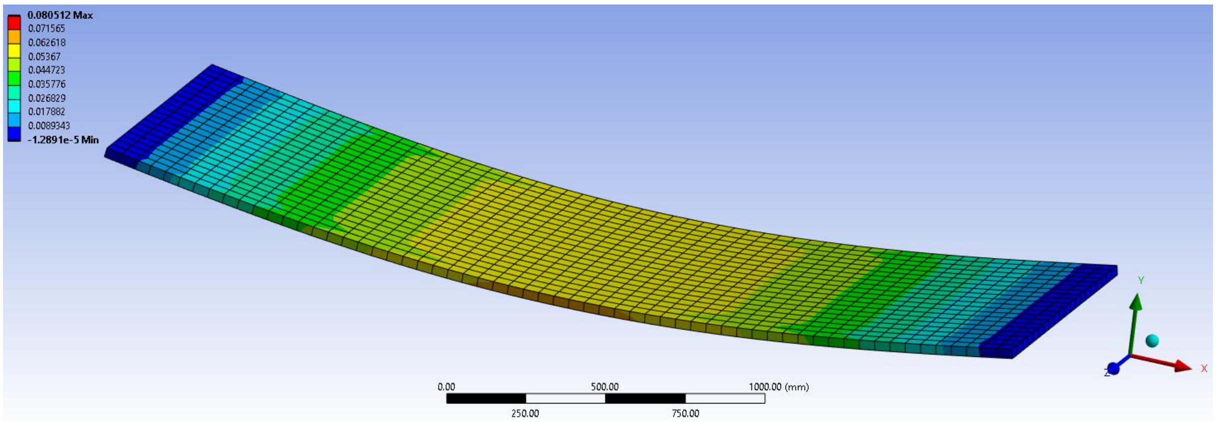

(d) Composite part of Reinforced slab tension stress

Figure 8. Maximum principal stress

Values of deflexion and stresses are indicated in Table 6. The deflexion decreases when the aged concrete increases from 20 to 45 GPa. The deflexion of 15 GPa concrete reinforced aged slab is equivalent to 17 GPa concrete non-reinforced slab. The recycled composite improves the slab deflexion when used as reinforcement. The results for stresses are more interesting: for 15 GPa concrete, the stress for a reinforced slab on concrete is 0.238 MPa compared to an aged non-reinforced slab, which is equal to 0.283 MPa.

Table 6. Deformations and stresses of non-reinforced and reinforced slabs as a function of concrete young's modulus

Concrete Young's Modulus [GPa]	Non-Reinf. Slab Deformation [mm]	Reinf. Slab Deformation [mm]	Non-Reinf. Slab Stress [MPa]	Reinf Slab Stress [MPa]	Reinf Slab-Concrete Stress [MPa]	Reinf Slab-Composite Stress [MPa]
15	0.181	0.159	0.283	0.238	0.238	0.081
16	0.169	0.150	0.283	0.240	0.240	0.076
17	0.159	0.142	0.283	0.242	0.242	0.072
18	0.151	0.135	0.283	0.244	0.244	0.069
19	0.143	0.129	0.283	0.246	0.246	0.066
20	0.135	0.123	0.283	0.247	0.247	0.063
21	0.129	0.117	0.283	0.249	0.249	0.060
22	0.123	0.112	0.283	0.250	0.250	0.058
23	0.118	0.108	0.283	0.251	0.251	0.056
24	0.113	0.104	0.283	0.253	0.253	0.054
25	0.108	0.100	0.283	0.254	0.254	0.052
26	0.104	0.096	0.283	0.255	0.255	0.050
27	0.100	0.093	0.283	0.256	0.256	0.048
28	0.097	0.090	0.283	0.256	0.256	0.047
29	0.093	0.087	0.283	0.257	0.257	0.045
30	0.090	0.084	0.283	0.258	0.258	0.044
31	0.087	0.082	0.283	0.259	0.259	0.043
32	0.085	0.079	0.283	0.259	0.259	0.042
33	0.082	0.077	0.283	0.260	0.260	0.040
34	0.080	0.075	0.283	0.261	0.261	0.039
35	0.077	0.073	0.283	0.261	0.261	0.038
36	0.075	0.071	0.283	0.262	0.262	0.037
37	0.073	0.069	0.283	0.262	0.262	0.036
38	0.071	0.068	0.283	0.263	0.263	0.035
39	0.069	0.066	0.283	0.263	0.263	0.035
40	0.068	0.064	0.283	0.264	0.264	0.034
41	0.066	0.063	0.283	0.264	0.264	0.033
42	0.065	0.061	0.283	0.264	0.264	0.032
43	0.063	0.060	0.283	0.265	0.265	0.032
44	0.062	0.059	0.283	0.265	0.265	0.031
45	0.060	0.057	0.283	0.266	0.266	0.030

4. Conclusions

This study investigated the influence of random fiber distribution on the mechanical properties of CCP/PVC composites using the Mori-Tanaka, Halpin-Tsai, and finite element method models. The results showed that increasing the fiber volume fraction significantly enhances the composite's elastic moduli up to 101% according to the Halpin-Tsai model. Moreover, varying fiber orientation distribution improved mechanical properties by up to 15.56%. The effect of fiber length became negligible beyond an aspect ratio of 100, indicating an asymptotic behavior in stiffness enhancement. Additionally, the study explored the application of CCP/PVC composites for reinforcing aged concrete slabs. Finite element simulations demonstrated that integrating a CCP/PVC composite layer effectively reduced slab with Young's modulus of 15 GPa, when reinforced with composite, experienced a stress reduction of approximately 16% highlighting its suitability for structural reinforcement. Overall, this work confirms the mechanical viability and environmental benefits of CCP/PVC composites. By utilizing recycled materials, the proposed approach supports sustainability goals and contributes to lowering carbon emissions in the construction industry.

Conflict of Interest

The corresponding author states that there is no conflict of interest on behalf of all authors.

Acknowledgements

This work is being developed as part of project 22PEJC-D6P5, which aims to encourage young researchers. The Ministry of Higher Education and Research of Tunisia financed and supported the project.

Data Availability Statement

Not applicable.

REFERENCES

[1] L. Tams, T. Nehls, and C. S. C. Calheiros, “Rethinking green roofs- natural and recycled materials improve their carbon footprint,” *Build. Environ.*, vol. 219, p. 109122, Jul. 2022, doi: 10.1016/j.buildenv.2022.109122.

[2] G. A. Blengini, “Life cycle of buildings, demolition and recycling potential: A case study in Turin, Italy,” *Build. Environ.*, vol. 44, no. 2, pp. 319–330, Feb. 2009, doi: 10.1016/j.buildenv.2008.03.007.

[3] H. Monteiro, I. Ribeiro, M. Gonçalves, M. Iten, and N. S. Caetano, “Life cycle energy and carbon analysis of a road-safety barrier produced using recycled tire rubber,” *Energy Rep.*, vol. 8, pp. 270–276, Jun. 2022, doi: 10.1016/j.egyr.2022.01.038.

[4] F. Ezzahra El Abbassi, M. Assarar, R. Ayad, H. Sabhi, S. Buet, and N. Lamdouar, “Effect of Recycling Cycles on the Mechanical and Damping Properties of Short Alfa Fibre Reinforced Polypropylene Composite,” *J. Renew. Mater.*, vol. 7, no. 3, pp. 253–267, 2019, doi: 10.32604/jrm.2019.01759.

[5] H. Mechakra, A. Nour, S. Lecheb, and A. Chellil, “Mechanical characterizations of composite material with short Alfa fibers reinforcement,” *Compos. Struct.*, vol. 124, pp. 152–162, Jun. 2015, doi: 10.1016/j.compstruct.2015.01.010.

[6] S. L. Omairey, P. D. Dunning, and S. Sriramula, “Development of an ABAQUS plugin tool for periodic RVE homogenisation,” *Eng. Comput.*, vol. 35, no. 2, pp. 567–577, Apr. 2019, doi: 10.1007/s00366-018-0616-4.

[7] C. Chen *et al.*, “Comparative analysis of natural fiber reinforced polymer and carbon fiber reinforced polymer in strengthening of reinforced concrete beams,” *J. Clean. Prod.*, vol. 263, p. 121572, Aug. 2020, doi: 10.1016/j.jclepro.2020.121572.

[8] S. Helaili, T. Rezgui, A. Guizani, and F. Najjar, “Reinforcement of Load-Bearing Structural Elements by Curved Composite Plates Made from Braided Natural Fibers,” in *Design and Modeling of Mechanical Systems - V*, L. Walha, A. Jarraya, F. Djemal, M. Chouchane, N. Aifaoui, F. Chaari, M. Abdennadher, A. Benamara, and M. Haddar, Eds., in Lecture Notes in Mechanical Engineering. , Cham: Springer International Publishing, 2023, pp. 171–178. doi: 10.1007/978-3-031-14615-2_20.

[9] S. Helaili, A. Guizani, F. Najar, and M. Chafra, “Novel Rebar Made from Epoxy and Braided Natural Alfa Fibers,” in *Design and Modeling of Mechanical Systems - V*, L. Walha, A. Jarraya, F. Djemal, M. Chouchane, N. Aifaoui, F. Chaari, M. Abdennadher, A. Benamara, and M. Haddar, Eds., in Lecture Notes in Mechanical Engineering. , Cham: Springer International Publishing, 2023, pp. 188–194. doi: 10.1007/978-3-031-14615-2_22.

[10] S. Helaili, S. Bouajila, H. Kaddami, and M. Chafra, “Turbine Blade Made of Natural Fiber Composite Structural and Vibrational Behavior,” in *Design and Modeling of Mechanical Systems - V*, L. Walha, A. Jarraya, F. Djemal, M. Chouchane, N. Aifaoui, F. Chaari, M. Abdennadher, A. Benamara, and M. Haddar, Eds., in Lecture Notes in Mechanical Engineering. , Cham: Springer International Publishing, 2023, pp. 743–749. doi: 10.1007/978-3-031-14615-2_83.

[11] S. Helaili and M. Chafra, “Identification of mechanical properties of a braided alfa stem (Stipa tenacissima L.) by an inverse method,” *J. Compos. Mater.*, vol. 57, pp. 443–450, 2023, doi: 10.1177/00219983221147685.

[12] I. Ráthy *et al.*, “Preparation and characterization of poly(vinyl chloride)-continuous carbon fiber composites,” *J. Appl. Polym. Sci.*, vol. 124, no. 1, pp. 190–194, Apr. 2012, doi: 10.1002/app.33617.

[13] E. Mahdi and A. Dean, “The Effect of Filler Content on the Tensile Behavior of Polypropylene/Cotton Fiber and poly(vinyl chloride)/Cotton Fiber Composites,” *Materials*, vol. 13, no. 3, p. 753, Feb. 2020, doi: 10.3390/ma13030753.

[14] L. Chazeau, J. Y. Cavaill, G. Canova, R. Dendievel, and B. Boutherin, “Viscoelastic properties of plasticized PVC reinforced with cellulose whiskers,” *J. Appl. Polym. Sci.*, vol. 71, no. 11, pp. 1797–1808, Mar. 1999, doi: 10.1002/(SICI)1097-4628(19990314)71:11<1797::AID-APP9>3.0.CO;2-E.

[15] M. Nachtane, F. Meraghni, G. Chatzigeorgiou, L. T. Harper, and F. Pelascini, “Multiscale viscoplastic modeling of recycled glass fiber-reinforced thermoplastic composites: Experimental and numerical investigations,” *Compos. Part B Eng.*, vol. 242, p. 110087, Aug. 2022, doi: 10.1016/j.compositesb.2022.110087.

[16] M. Nodehi, “Epoxy, polyester and vinyl ester based polymer concrete: a review,” *Innov. Infrastruct. Solut.*, vol. 7, no. 1, p. 64, Feb. 2022, doi: 10.1007/s41062-021-00661-3.

[17] J. Haloi, A. C. Borsaikia, and K. D. Singh, "Mechanical characterization of pultruded GFRP channel, wide flange and rectangular hollow profiles," *Innov. Infrastruct. Solut.*, vol. 7, no. 1, p. 21, Feb. 2022, doi: 10.1007/s41062-021-00501-4.

[18] H. A. Khalil, M. Tehrani, Y. Davoudpour, A. Bhat, M. Jawaid, and A. Hassan, "Natural fiber reinforced poly(vinyl chloride) composites: A review," *J. Reinf. Plast. Compos.*, vol. 32, no. 5, pp. 330–356, Mar. 2013, doi: 10.1177/0731684412458553.

[19] S. Tungjitpornkull, K. Chaochanchaikul, and N. Sombatsompop, "Mechanical Characterization of E-Chopped Strand Glass Fiber Reinforced Wood/PVC Composites," *J. Thermoplast. Compos. Mater.*, vol. 20, no. 6, pp. 535–550, Nov. 2007, doi: 10.1177/0892705707084541.

[20] S. Tungjitpornkull and N. Sombatsompop, "Processing technique and fiber orientation angle affecting the mechanical properties of E-glass fiber reinforced wood/PVC composites," *J. Mater. Process. Technol.*, vol. 209, no. 6, pp. 3079–3088, Mar. 2009, doi: 10.1016/j.jmatprotec.2008.07.021.

[21] F. Mengeloglu and L. M. Matuana, "Mechanical properties of extrusion-foamed rigid PVC/wood-flour composites," *J. Vinyl Addit. Technol.*, vol. 9, no. 1, pp. 26–31, Mar. 2003, doi: 10.1002/vnl.10058.

[22] N. Mongkollapkit, A. Kositchaiyong, V. Rosarpitak, and N. Sombatsompop, "Mechanical and morphological properties for sandwich composites of wood/PVC and glass fiber/PVC layers," *J. Appl. Polym. Sci.*, vol. 116, no. 6, pp. 3427-3436, 2010, doi: 10.1002/app.31882.

[23] N. Patel and P. Jain, "An investigation on mechanical properties in randomly oriented short natural fiber reinforced composites," *Mater. Today Proc.*, vol. 37, pp. 469–479, 2021, doi: 10.1016/j.matpr.2020.05.452.

[24] Z. Li, Z. Liu, Z. Lei, and P. Zhu, "An innovative computational framework for the analysis of complex mechanical behaviors of short fiber reinforced polymer composites," *Compos. Struct.*, vol. 277, p. 114594, Dec. 2021, doi: 10.1016/j.compstruct.2021.114594.

[25] M. H. Abd-Elrahman, I. S. Agwa, Y. Elsakhawy, and M. S. Rizk, "Effect of utilising ferrosilicon and recycled steel fibres on ultra-high-strength concrete containing recycled granite," *Case Stud. Constr. Mater.*, vol. 18, p. e01903, Jul. 2023, doi: 10.1016/j.cscm.2023.e01903.

[26] M. Saad, I. S. Agwa, B. Abdelsalam Abdelsalam, and M. Amin, "Improving the brittle behavior of high strength concrete using banana and palm leaf sheath fibers," *Mech. Adv. Mater. Struct.*, vol. 29, no. 4, pp. 564–573, Feb. 2022, doi: 10.1080/15376494.2020.1780352.

[27] M. S. Fattouh, B. A. Tayeh, I. S. Agwa, and E. K. Elsayed, "Improvement in the flexural behaviour of road pavement slab concrete containing steel fibre and silica fume," *Case Stud. Constr. Mater.*, vol. 18, p. e01720, Jul. 2023, doi: 10.1016/j.cscm.2022.e01720.

[28] M. Amin, A. A. Hakamy, A. M. Zeyad, B. A. Tayeh, and I. S. Agwa, "Improving the brittle behavior of high-strength shielding concrete blended with lead oxide, bismuth oxide, and tungsten oxide nanoparticles against gamma ray," *Struct. Eng. Mech.*, vol. 85, no. 1, pp. 29–53, Jan. 2023, doi: 10.12989/SEM.2023.85.1.029.

[29] K. Abdelsamie, I. S. Agwa, B. A. Tayeh, and R. D. A. Hafez, "Improving the brittle behaviour of high-strength concrete using keratin and glass fibres," *Adv. Concr. Constr.*, vol. 12, no. 6, pp. 469–477, Dec. 2021, doi: 10.12989/ACC.2021.12.6.469.

[30] A. M. Zeyad, I. Y. Hakeem, M. Amin, B. A. Tayeh, and I. S. Agwa, "Effect of aggregate and fibre types on ultra-high-performance concrete designed for radiation shielding," *J. Build. Eng.*, vol. 58, p. 104960, Oct. 2022, doi: 10.1016/j.jobe.2022.104960.

[31] M. Amin, I. Y. Hakeem, A. M. Zeyad, B. A. Tayeh, A. M. Maglad, and I. S. Agwa, "Influence of recycled aggregates and carbon nanofibres on properties of ultra-high-performance concrete under elevated temperatures," *Case Stud. Constr. Mater.*, vol. 16, p. e01063, Jun. 2022, doi: 10.1016/j.cscm.2022.e01063.

[32] A. A. J. Ghanim, M. Amin, A. M. Zeyad, B. A. Tayeh, I. S. Agwa, and Y. Elsakhawy, "Effect of polypropylene and glass fiber on properties of lightweight concrete exposed to high temperature," *Adv. Concr. Constr.*, vol. 15, no. 3, pp. 179–190, Mar. 2023, doi: 10.12989/ACC.2023.15.3.179.

[33] Y. W. Leong, M. B. Abu Bakar, Z. A. Mohd. Ishak, A. Ariffin, and B. Pukanszky, "Comparison of the mechanical properties and interfacial interactions between talc, kaolin, and calcium carbonate filled polypropylene composites," *J. Appl. Polym. Sci.*, vol. 91, no. 5, pp. 3315–3326, Mar. 2004, doi: 10.1002/app.13542.

[34] Alphagary, "PVC - general purpose - DURAL® GRE222 Technical Datasheet Supplied by Alphagary." [Online]. Available:https://www.alphagary.com/product/gre222gre222

[35] S. A. Malak, "Tensile stress strain model of polyvinyl chloride/calcium carbonate (PVC/$CaCO_3$) nanocomposite plank," *Results Mater.*, vol. 10, p. 100193, Jun. 2021, doi: 10.1016/j.rinma.2021.100193.

[36] J. C. Halpin, "Effects of Environmental Factors on Composite Materials.," *Mater. Sci.*, vol. 67, p. 62, 1969.

[37] Z.-M. Huang, W.-J. Guo, H.-B. Huang, and C.-C. Zhang, "Tensile Strength Prediction of Short Fiber Reinforced Composites," *Materials*, vol. 14, no. 11, p. 2708, May 2021, doi: 10.3390/ma14112708.

[38] H. Berger, S. Kari, U. Gabbert, R. Rodríguez Ramos, J. Bravo Castillero, and R. Guinovart Díaz, "Evaluation of effective material properties of randomly distributed short cylindrical fiber composites using a numerical homogenization technique," *J. Mech. Mater. Struct.*, vol. 2, no. 8, pp. 1561–1570, Oct. 2007, doi: 10.2140/jomms.2007.2.1561.

[39] Y. S. Mohamed and A. Abdelbary, "Theoretical and experimental study on the influence of fiber orientation on the tensile properties of unidirectional carbon fiber/epoxy composite," *Alex. Eng. J.*, vol. 67, pp. 693–705, Mar. 2023, doi: 10.1016/j.aej.2022.12.058.

[40] A. Ionita and Y. J. Weitsman, "Randomly reinforced composites: properties, failure and aspects of material design," *Probabilistic Eng. Mech.*, vol. 21, no. 1, pp. 64–72, Jan. 2006, doi: 10.1016/j.probengmech.2005.07.006.

[41] R. Chammas, O. Abraham, P. Cote, H. A. Pedersen, and J. F. Semblat, "Characterization of Heterogeneous Soils Using Surface Waves: Homogenization and Numerical Modeling," *Int. J. Geomech.*, vol. 3, no. 1, pp. 55–63, Sep. 2003, doi: 10.1061/(ASCE)1532-3641(2003)3:1(55).